Int J Adv Manuf Technol (2017) 90:141–151
DOI 10.1007/s00170-016-9383-9

ORIGINAL ARTICLE

# Friction stir vibration welding process: modified version of friction stir welding process

M. Rahmi [1] · Mahmoud Abbasi [1]

Received: 17 May 2016 / Accepted: 22 August 2016 / Published online: 27 August 2016


**Abstract** In the current research, a new method is applied to modify the conventional friction stir welding (FSW) process. Fixture, which fixes the workpieces, is shaken mechanically during FSW in a direction normal to weld line in order to increase the straining of weld region material. In other words, vibration of workpieces is accompanied by the rotating motion of tool. This new process can be described as friction stir vibration welding (FSVW). Al 5052 alloy specimens are welded by two welding methods, FSW and FSVW. Microstructure and mechanical properties of welded specimens are compared. Metallography analyses indicate that grain size decreases and hardness increases as FSVW method is applied. Tensile test results also show that strength and ductility values of friction stir vibration (FSV)-welded specimens are greater than those relating to friction stir (FS)-welded specimens. It is because of more work hardening of plasticized material, during FSVW, which leads to more generation and movement of dislocations. Correspondingly, grain size decreases and mechanical properties improve. Additionally, it is observed that the mechanical properties of the weld improve as vibration frequency increases.

**Keywords** Solid-state welding · Friction stir vibration welding · Microstructure · Mechanical properties

**Nomenclature**

| | |
|---|---|
| EDM | Electrical discharge machining |
| EFSW | Electrical current-aided friction stir welding |
| FSW | Friction stir welding |
| HAZ | Heat-affected zone |
| HABs | High angle boundaries |
| LAFSW | Laser-assisted friction stir welding |
| LAB | Low angle boundaries |
| TMAZ | Thermo-mechanical affected zone |
| UVeFSW | Ultrasonic vibration-assisted friction stir welding |
| WNZ | Weld nugget zone |
| a, b | Constants |
| EL | Elongation |
| k | Strengthening coefficient |
| Q | Activation energy |
| R | Gas constant |
| T | Temperature |
| UTS | Ultimate tensile strength |
| Z | Zener-Hollomon parameter |
| $\varepsilon$ | Strain rate |
| $\sigma$ | Strength |
| $\sigma_0$ | Friction stress |

✉ Mahmoud Abbasi
m.abbasi@aut.ac.ir

[1] Faculty of Engineering, University of Kashan, Ravandi Blvd, Kashan, Iran

## 1 Introduction

Solid-state welding is a welding process that produces bonding at temperatures essentially below the melting point of the base materials being joined [1]. These welding process offers certain advantages since the base metal does not melt and a nugget is formed. The metals being welded usually retain their original properties without the heat-affected zone problems involved when there is base metal melting. Furthermore, when dissimilar metals are joined, their thermal expansion and conductivity are of much less importance with solid-state welding processes than with the fusion welding processes [2, 3].

Friction stir welding (FSW) is relatively a new solid-state welding process. This welding technique is energy efficient, versatile, and environment friendly [1, 4]. In particular, it can be used to join high-strength aerospace aluminum alloys and other metallic alloys that are hard to weld by conventional fusion welding [5, 6]. FSW eliminates many of the defects associated with conventional fusion welding techniques such as shrinkage, solidification cracking, and porosity [7, 8]. The bond between the two pieces is made solely of the original materials. It usually results in similar strength, bending, and fatigue characteristics of the parent materials. FSW uses a non-consumable rotating tool consisted of pin and shoulder to join two facing surfaces. Tool is inserted into the abutting edges of sheets or plates to be joined and traversed along the line of joint. Heat is generated between the tool and material which leads to a very soft region near the tool. The tool mixes mechanically the softened regions of two pieces of metal at the place of the joint [9].

However, some disadvantages of the FSW have been identified. Exit hole left when tool is withdrawn, large down forces required with heavy-duty clamping necessary to hold specimens, little flexibility, and slow traverse rate are some of these concerns. Large forces on tool might result in tool fracture and maximize wear of tool. Various trials have been carried out by researchers to modify FSW process to get better characteristics of friction stir (FS)-welded specimens, increase tool life, and decrease the energy consumption.

Kohn et al. [10] used laser beam as assistant heat source in FSW to join AZ9lD Mg alloy plates and found that the use of laser power lowered significantly the need to apply large forces both on the welding tool and the workpiece. Casalino et al. [11] combined laser system and FSW machine. Laser power was used to preheat and to plasticize the volume of the workpiece ahead of the rotating tool. They applied an ytterbium fiber laser with maximum power of 4 kW during FSW process on 3 mm thick 5754H111 aluminum alloy plates in lap joint configuration. Their comparison between microstructure and hardness of conventionally welded specimens using FSW method with those welded by laser-assisted friction stir welding (LAFSW) showed that grain refinement and the mechanical properties of joints were improved by application of LAFSW.

Sun et al. [12] considered the modification of FSW by applying a high current frequency induction method to preheat low carbon steel plates with thickness of 1.6 mm before welding. It was found that the applied load significantly decreased when the preheating was adopted. The welds showed a high failure load and they fractured through the plug mode.

Luo et al. [13] introduced electrical current-aided FSW (EFSW) as a hybrid welding technology. In this method, electric current flows from the FSW tool through the contact interface into the workpieces. They investigated the effect of EFSW and electric current intensity on welding seam of AZ31 B and Al 7075 joints. The results revealed EFSW refined grain size significantly and increased the hardness in the weld nugget zone (WNZ) of AZ31B joints, while for the Al 7075 joints, the grain size in the WNZ and heat affected zone (HAZ) increased lightly with the increase in electric current intensity. Liu et al. [14] applied another version of EFSW method. In their technique, two additional copper brushes, without requiring the tool to be one of the electrodes, were pressed against the top surface of the workpiece. These copper brushes, serving as the anode and cathode, were mounted to the spindle holder and traveled together with the FSW tool. Using this technique, Al 6061 was joined to TRIP 780 steel. They found that axial welding force was reduced and formation of thin layer of intermetallic compounds at the Al-Fe interface enhanced. They concluded that the combined effect of accelerated atom diffusion and reduced activation energy for chemical reaction because of joule resistance heating were the reasons for improvements.

Liu et al. [15] applied a sonotrode to transmit the ultrasonic energy directly into the localized area of the workpiece near and ahead of the rotating tool during FSW. They called this process ultrasonic vibration-assisted friction stir welding (UVeFSW). They investigated the influence of ultrasonic vibration on microstructure and mechanical properties of butt-welded 2024Al-T4 joints. Morphology inspection, X-ray detection, and metallographic inspection of the welds revealed that the stir zone in the UVeFSW broadened, while the grains in the heat-affected zone had no obvious growth. Mechanical test results indicated that by application of UVeFSW, the tensile strength and elongation of joints, as well as the microhardness value in the stir zone increased. Amini and Amiri [16] studied the effect of ultrasonic vibrations on tool force and temperature as well as tensile strength and hardness of the weld region formed by FSW. Ultrasonic vibrations were employed on the tool in pin direction and perpendicular to the welding direction, and AA6061-T6 specimens were joined. They found that application of ultrasonic vibration during FSW decreased the downward force of tool and increased the strength and ductility of weld region.

The problem in regard with UVeFSW is high cost of equipment, namely ultrasonic generator and transducer, and its application which is not easy. In the current research, unlike conventional UVeFSW, in which the tool is vibrated by ultrasonic, the workpiece is vibrated mechanically in a direction normal to weld line. In fact, in the developed method which is easy to apply, the workpieces are vibrated during FSW. The microstructure and mechanical properties of weld developed by the modified welding process are compared with those of weld resulted from conventional FSW process.

## 2 Materials and methods

Al 5052 sheet metal with thickness of 3 were used as work material. Chemical composition of the studied material is presented in Table 1.

Rectangular specimens with size of 120 × 50 (mm × mm) were cut from the studied sheet metal. The longitudinal edges of specimens were cleaned of oil and debris carefully, and they were aligned along the cleaned edges to be in a butt weld position on fixture (Fig. 1). Oil removal was carried out by rinsing the specimens by a caustic solution of sodium hydroxide and water. They were dried by cloth finally.

Vibration was applied through fixture. Schematic design of the method utilized to vibrate the fixture is illustrated in Fig. 2. In this design, rotation movement of motor shaft is transformed to linear motion of fixture using a camshaft. The power for fixture vibration was supplied by an AC motor 0.5 kW. The motor was equipped by a driver to bring the possibility to change the motor rotation speed. Camshaft was designed in a way that it resulted in vibration of fixture with amplitude of 0.5 mm.

Tool was consisted of a cylindrical shoulder and a trapezoidal pin. Pin was made of tungsten carbide, and the shoulder was prepared from M2 steel. Shoulder hardness after heat treatment was 65 HRC. In order to study the effect of shoulder size on microstructure and mechanical properties, two shoulders with different sizes were used. Small shoulder with diameter of 22 mm and large shoulder with diameter of 32 mm were applied. Except the diameter, the geometries for both shoulders were the same. The geometry for FSW tool with small shoulder is presented in Fig. 3. The penetration depth of pin was 2.8 mm.

To find the effect of the developed welding method on microstructure and mechanical properties, different welding conditions were applied. These conditions are presented in Table 2. For each condition, both welding processes, FSW and FSVW, were done. Vibration frequency was 16.67 Hz. However, to get the effect of vibration frequency on mechanical properties, some specimens were also welded by frequency of 13.33 and 19.17 Hz.

**Table 1** Chemical composition of the studied material (wt.%)

| Al | Cr | Cu | Fe | Mg | Mn | Si | Zn | Other |
|---|---|---|---|---|---|---|---|---|
| Balance | 0.25 | 0.1 | 0.35 | 2.4 | 0.1 | 0.2 | 0.1 | 0.15 |

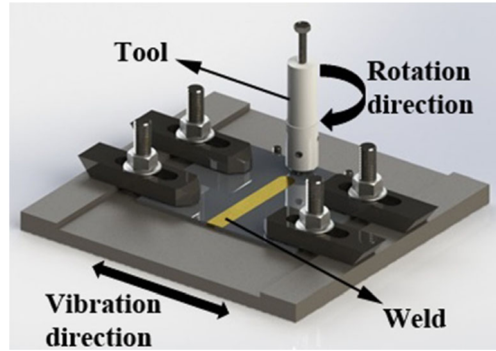


**Fig. 1** Schematic design of fixture used for fastening the specimens

The microstructure and mechanical properties of the welded specimens were analyzed. Metallography samples were prepared from the cross sections of the welded specimens, and they were subjected to grinding, polishing, and etching. The test sections were mounted and manually grinded with emery papers (80–2400 mesh) and carefully polished using alumina powders with size of 0.03 μm. Metallographic samples were etched for 5 s with an etchant consisting of 2.58 vol.% picric acid, 10.82 vol.% acetic acid, 10.82 vol.% water, and 75.78 vol.% ethanol.

The grain size was evaluated by optical microscopy, and it was quantified through the mean linear intercept method (ASTM E-112 [17]). To measure the grain size, a square of selected area (300 × 300 $\mu m^2$) was overlaid on a micrograph and the number of grains including the grains completely within the known area plus one half of the number of grains intersected by the circumference of the area were counted. Accordingly, the number of grains per unit area was calculated and then, the average diameter of the grains was estimated assuming the grains to be spherical in shape.

Sub-size samples for tensile testing based on the ASTM-E8 standard test were prepared according to ref. [18]. The samples were obtained from the welded specimens using wire electrical discharge machining (EDM) method in such a way that the weld was positioned in the middle of the gauge section. The schematic design of the tensile test sample is presented in Fig. 4. During the tensile test, the strain was measured using extensometer and the crosshead speed was

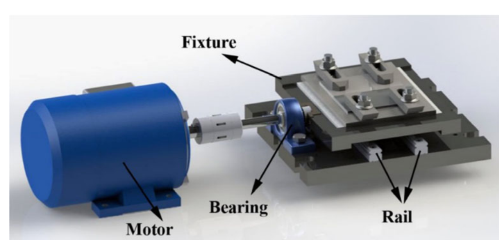


**Fig. 2** Schematic design of fixture and the set used for vibration

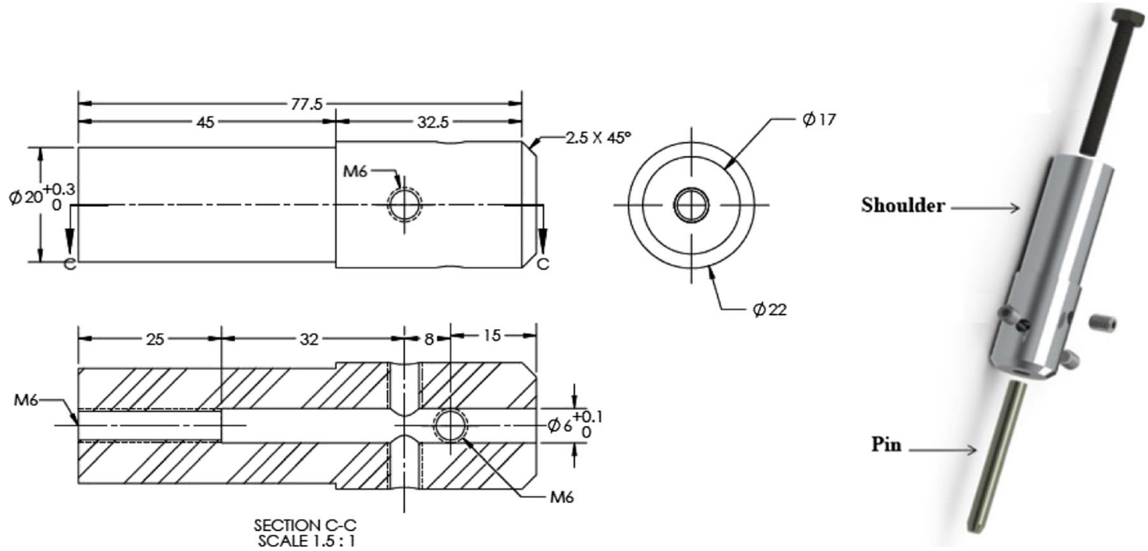


**Fig. 3** Geometry of pin and shoulder used for FSW and FSVW processes

5 mm min$^{-1}$. For each welding condition, three samples were tested.

Hardness was investigated using Vickers hardness test (HV) method. Microhardness tests were performed on polished samples using a programmable hardness test machine. The load was 1 N and the dwell time was 10 s. The mean value of 3 measurements was collected for each welding condition.

## 3 Results and discussion

### 3.1 Microstructure

Microstructures of welded specimens relating to different welding conditions, based on Table 2, as well as the base material are presented in Fig. 5. The weld region microstructures of welded specimens, at higher magnification, are presented in Fig. 6. The figures show the effect of vibration on microstructure and grain size for two shoulder sizes. Grain size measurement data for different welding conditions, relating to Fig. 6, are presented in Fig. 7. It is observed that vibration during welding decreases the grain size of weld region for both shoulders; additionally, grain sizes of specimens welded with small diameter shoulder are generally lower than those welded by large shoulder.

**Table 2** Different conditions were applied for welding

| Shoulder | Rotation speed (rpm) | Transverse speed (mm/min) | Vibration |
|---|---|---|---|
| Small | 1200 | 25 | − |
| | | | + |
| Large | 1200 | 25 | − |
| | | | + |

− and + stands denote without and with vibration, respectively

It is known that metal working during FSW results in dislocation generation in microstructure [19, 20]. Additionally, the heat produced during FSW, because of friction, brings the possibility to develop the dynamic recrystallization [21]. These result in formation of fine grains in the weld region. The authors believe that when tool stirring is accompanied by vibration of workpieces, during FSVW, strain and strain rate increase and more dislocations are generated and correspondingly finer grains develop in the weld region. This is in agreement with Zener-Hollomon relation [22].

$$Z = \varepsilon \exp\left(\frac{Q}{\mathrm{RT}}\right) \quad (1)$$

According to Zener-Hollomon relation (Eq. 1), $Z$ parameter increases as strain rate ($\varepsilon$ ) increases. Based on Eq. 2, which indicates the relation developed between Zener-Hollomon parameter ($Z$) and grain size ($D$) [23]:

$$D^{-1} = a\ln Z - b \quad (2)$$

grain size decreases, as $Z$ parameter increases.

Grain size enhancement, because of shoulder diameter increase, can be related to the effect of friction heat.

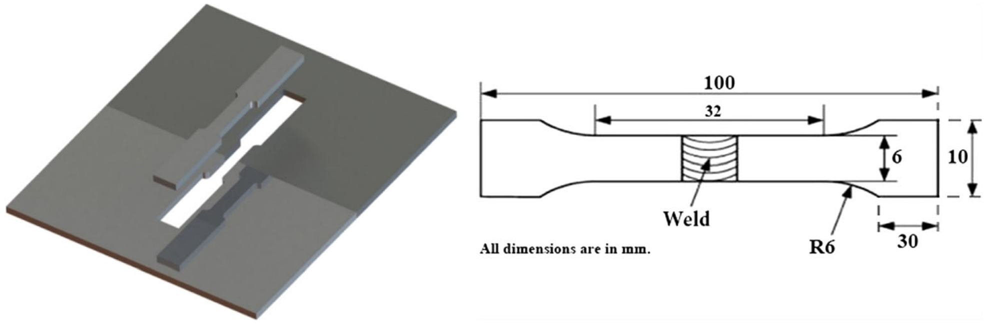


**Fig. 4** The schematic design of the tensile test sample prepared by electrical discharge machining (wire cut)

Researchers have found that more heat is produced during welding when shoulder diameter increases [24, 25]. Abbasi et al. [26] found that grain size increased as generated heat during FSW enhanced.

### 3.2 Mechanism of grain size refinement

It has been known that severe plastic deformation during FSW results in high density of dislocations [27, 28]. When vibration

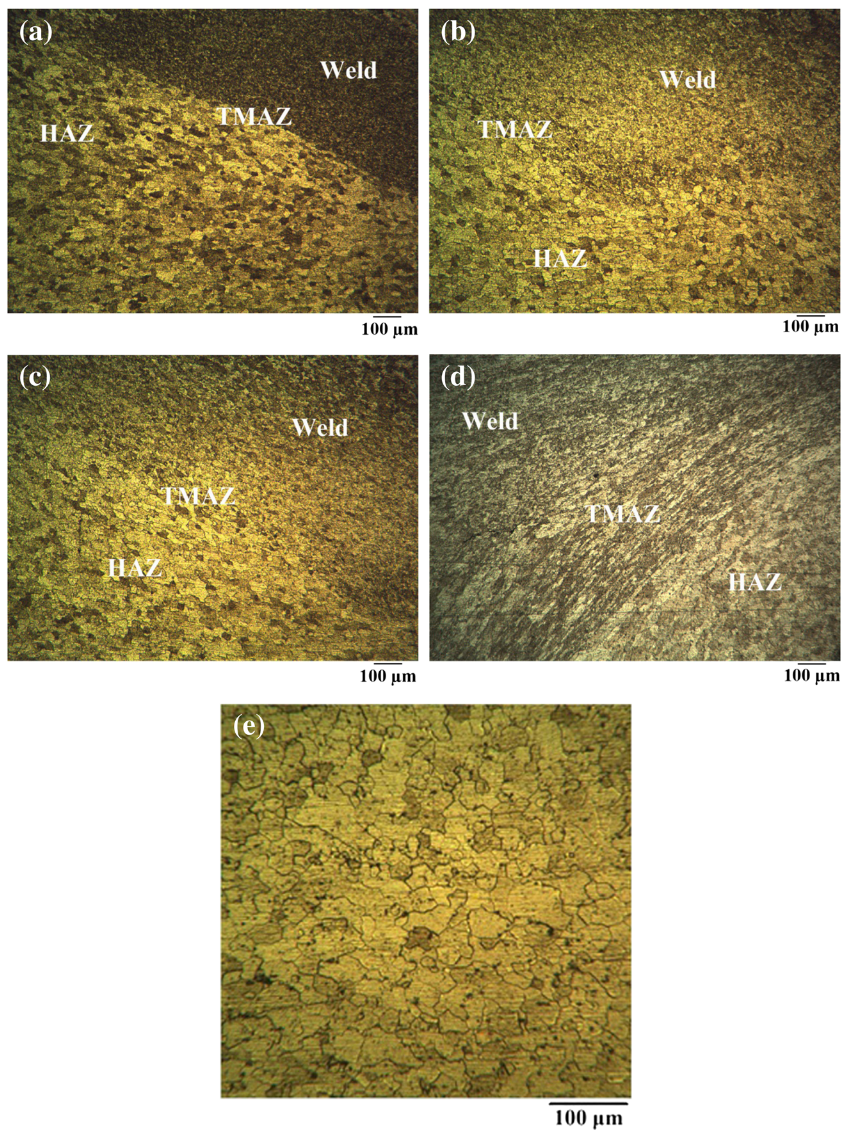


**Fig. 5** Microstructure of joints developed using different welding conditions as well as the base material: **a** FSVW with small diameter shoulder, **b** FSW with small diameter shoulder, **c** FSVW with large diameter shoulder, **d** FSW with large diameter shoulder, and **e** base material (welding parameters values were according to Table 2)

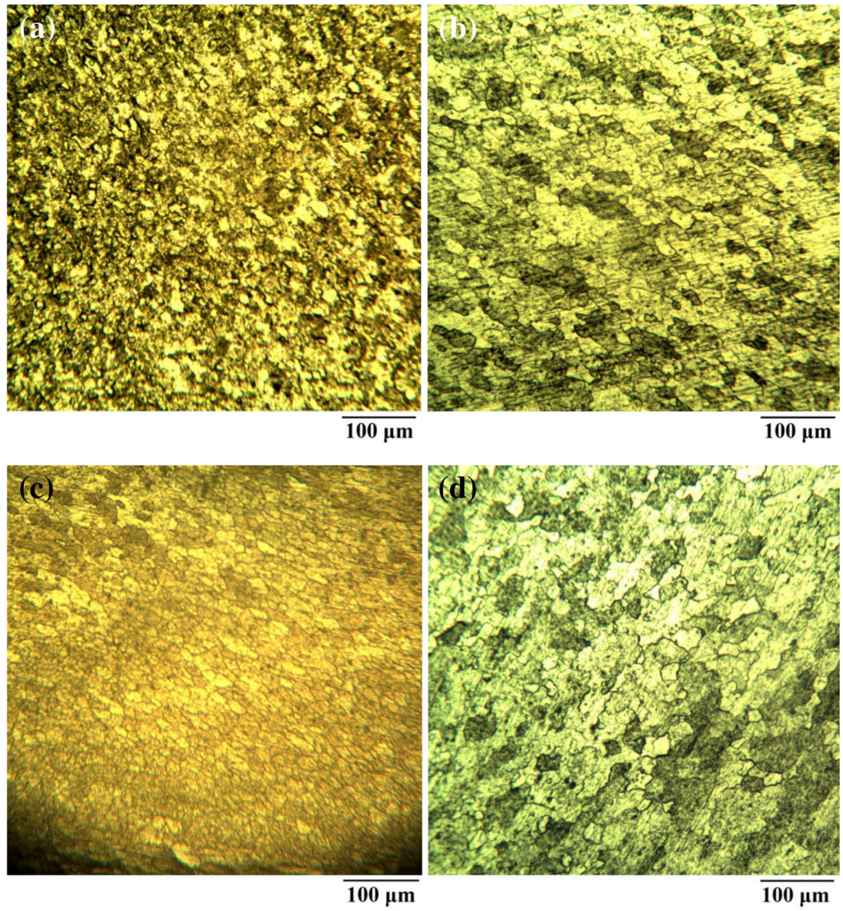


**Fig. 6** Weld region microstructure of FSV-welded specimens under different conditions: **a** FSVW with small diameter shoulder, **b** FSW with small diameter shoulder, **c** FSVW with large diameter shoulder, **d** FSW with large diameter shoulder (welding parameters values were according to Table 2)

is applied during FSW, plastic deformation and generation of dislocations increase and therefore, microstructure evolution proceeds faster. According to Kaibyshev [29], the microstructure evolution during severe plastic deformation consists of two sequential processes: (i) the formation of three-dimensional arrays of low angle boundaries (LABs) and (ii) the gradual transformation of LABs into high angle boundaries (HABs) (≥15°).

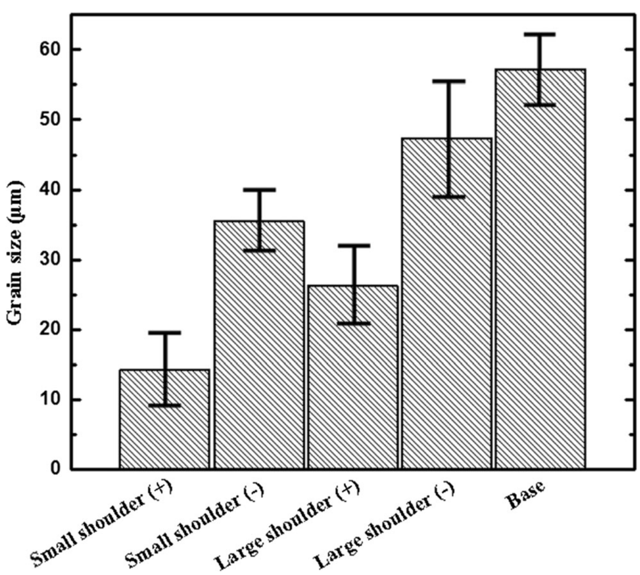


**Fig. 7** Weld region grain size data for different specimens welded using different welding conditions (welding parameters values were according to Table 2; *minus sign* and *plus sign* denote without and with vibration, respectively)

LABs with a low misorientation (~1°) are continuously formed in pure aluminum and its alloys by dynamic recovery during deformation by rearrangement of accumulating lattice dislocations (Fig. 8a). At high strain values, mobile dislocations move across sub-grains and are trapped by sub-boundaries resulting in an increase in their misorientation. Extensive rotation of sub-grains provides increasing misorientation of LABs with strain within sub-grains. These processes result in the formation of individual segments of HABs, and this can be considered as a proof for the occurrence of dynamic recrystallization (Fig. 8b). The recrystallized grains persistently replace sub-grains evolved at small strains through continuous transformation of their boundaries, and accordingly, grain size refinement occurs [30].

### 3.3 Mechanical properties

Stress-strain curves of welded specimens with vibration are compared with those welded without vibration in Fig. 9.

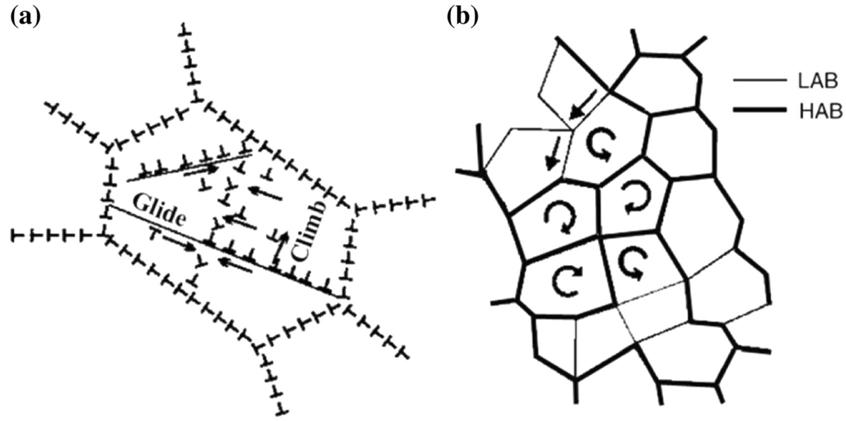


**Fig. 8** Schematic illustration of dynamic recrystallization: **a** dynamic recovery and formation of LABs and **b** grain size refinement due to gradual transformation of LABs into HABs [29]

Ultimate tensile strength and elongation at fracture of these specimens are presented in Table 3. Based on Table 3, strength and ductility values of FS-welded specimens with vibration are higher than those welded without vibration. Moreover, strength and ductility values of FS-welded specimens with small diameter shoulder are greater than those relating to large diameter shoulder. These can be related to the grain size effect, and they can be justified based on Hall-Petch relation [31]. According to this relation (Eq. 3), strength ($\sigma$) increases as grain size decreases. As vibration decreases the grain size ($D$) (Fig. 6), the strength of FS-welded specimens with vibration is generally higher than those welded without vibration.

$$\sigma = \sigma_0 + kD^{-\frac{1}{2}} \quad (3)$$

Various researches have been carried out to find the effect of grain size on ductility. Findings have shown that ductility increases as grain size decreases [32, 33]. As grain size decreases, grain boundary volume fraction increases. Grain boundaries act as obstacles for crack growth and enhance the ductility. Estrin et al. [33] noted the possibility of ductility enhancement in AZ31 magnesium alloy due to the transition in the fracture mechanism from intergranular fracture to transgranular fracture as grain size decreases. It is also observed in Fig. 9 that stress-strain curves of FS-welded specimens with small diameter shoulder are higher than those welded with large diameter shoulder.

Fractography analysis by SEM was carried out to compare the fracture surface of FS-welded and FSV-welded specimens. For both conditions, rotation and traveling speeds were 1200 rpm and 25 mm/min, respectively, and small shoulder with 22 mm diameter was used for stirring. The results are presented in Fig. 10.

Both samples show fracture surfaces characterized with presence of voids which indicate a ductile fracture. It is known that in ductile fracture, extensive plastic deformation takes place before fracture and the basic steps before fracture are void formation, void coalescence, and

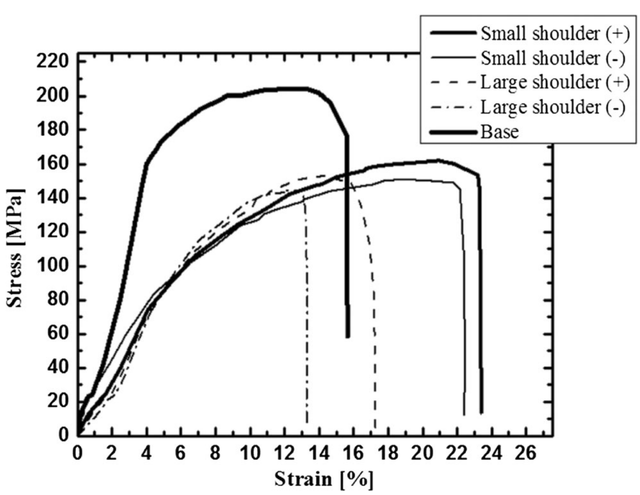


**Fig. 9** Stress-strain curves of base material, FS- and FSV-welded specimens (*minus sign* and *plus sign* denote without and with vibration, respectively)

**Table 3** Ultimate tensile strength and elongation at fracture of base material, FS-and FSV-welded specimens obtained from tensile test results presented in Fig. 9

| | Ultimate tensile strength (MPa) | Elongation (%) |
|---|---|---|
| Small shoulder (+) | 162.3 | 23.42 |
| Small shoulder (−) | 150.6 | 22.41 |
| Large shoulder (+) | 153.8 | 17.25 |
| Large shoulder (−) | 145.2 | 13.29 |
| Base | 204.1 | 15.64 |

− and + denote without and with vibration, respectively

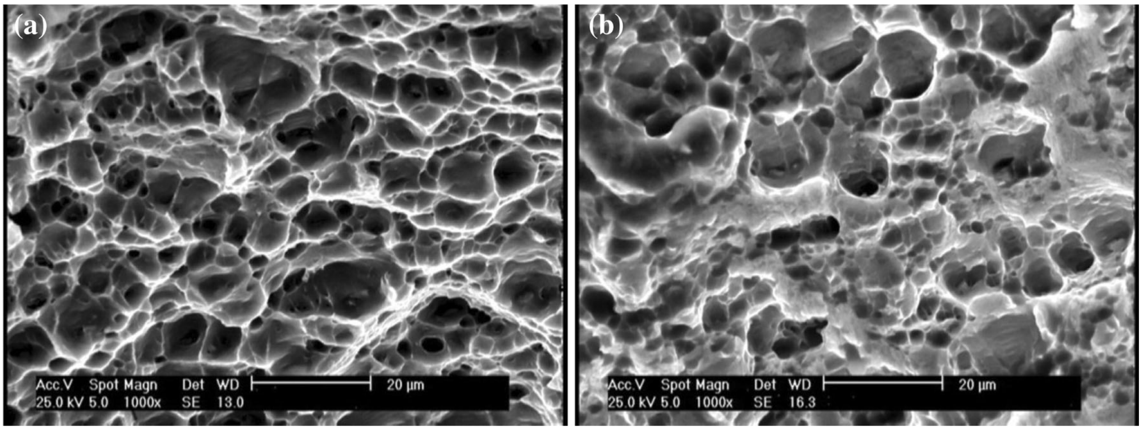


**Fig. 10** SEM fracture surface of **a** FSV-welded sample and **b** FS-welded sample

crack propagation [34, 35]. It is observed in Fig. 10 that the voids for FSV-welded sample are more than the other one. This indicates that FSV-welded sample has strained more than FS-welded sample before fracture. This is in agreement with tensile test results that ductility of FSV-welded samples is more than that of FS-welded sample.

Formability index values of FS-welded specimens are presented in Fig. 11. The formability index which is quantified with the UTS × EL relation, can be regarded as a fingerprint of energy absorption during tensile test, where UTS stands for ultimate tensile strength and EL stands for elongation [36]. It is observed in Fig. 11 that presence of vibration, during welding, increases the formability index. This can be related to the effect of vibration on strength and ductility of welded specimens which increases both.

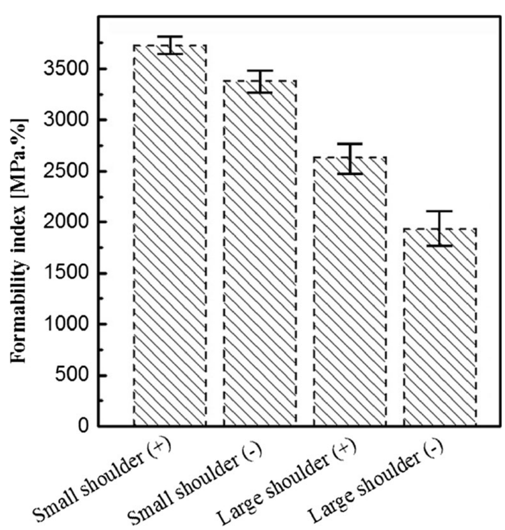


**Fig. 11** Formability indexes of FS- and FSV-welded specimens (*minus sign* and *plus sign* denote without and with vibration, respectively)

Hardness values of different zones of FSV-welded specimens are compared with FS-welded specimens, and the results are presented in Fig. 12. Figure 12 shows that weld and thermo-mechanical affected zone (TMAZ) region hardness of FSV-welded specimens are greater than those relating to FS-welded specimens, although HAZ hardness changes because vibration is small. This can be related to the effect of vibration on grain size. The presence of vibration during stirring refined the weld region grain size (Fig. 6), although it did not affect the HAZ grain size significantly (Fig. 5). It is known that grain size refinement is one of the strengthening mechanisms, and hardness increases as grain size decreases [37].

### 3.4 Effect of vibration frequency

The effect of vibration frequency on stress-strain curves of FSV-welded specimens is shown in Fig. 13. For all cases, the welding conditions, except frequency, were constant. Rotation speed was 1200 rpm, traveling speed was 25 mm/min, and shoulder with small diameter (22 mm) was applied for welding. It is observed in Fig. 13 that increment of frequency has increased the strength and ductility values.

This can be related to the effect of frequency on strain rate. Increase of frequency enhances the strain rate and correspondingly, according to Eqs. 2 and 3, Z increases and grain size ($D$) decreases. Hall-Petch relation (Eq. 3) indicates that strength and hardness increase as grain size decreases. Weld region hardness values of FSV-welded specimens with different vibration frequencies are presented in Fig. 14. As it is predicted, the greatest hardness value belongs to the FSV-welded specimen with the greatest amount of vibration frequency.

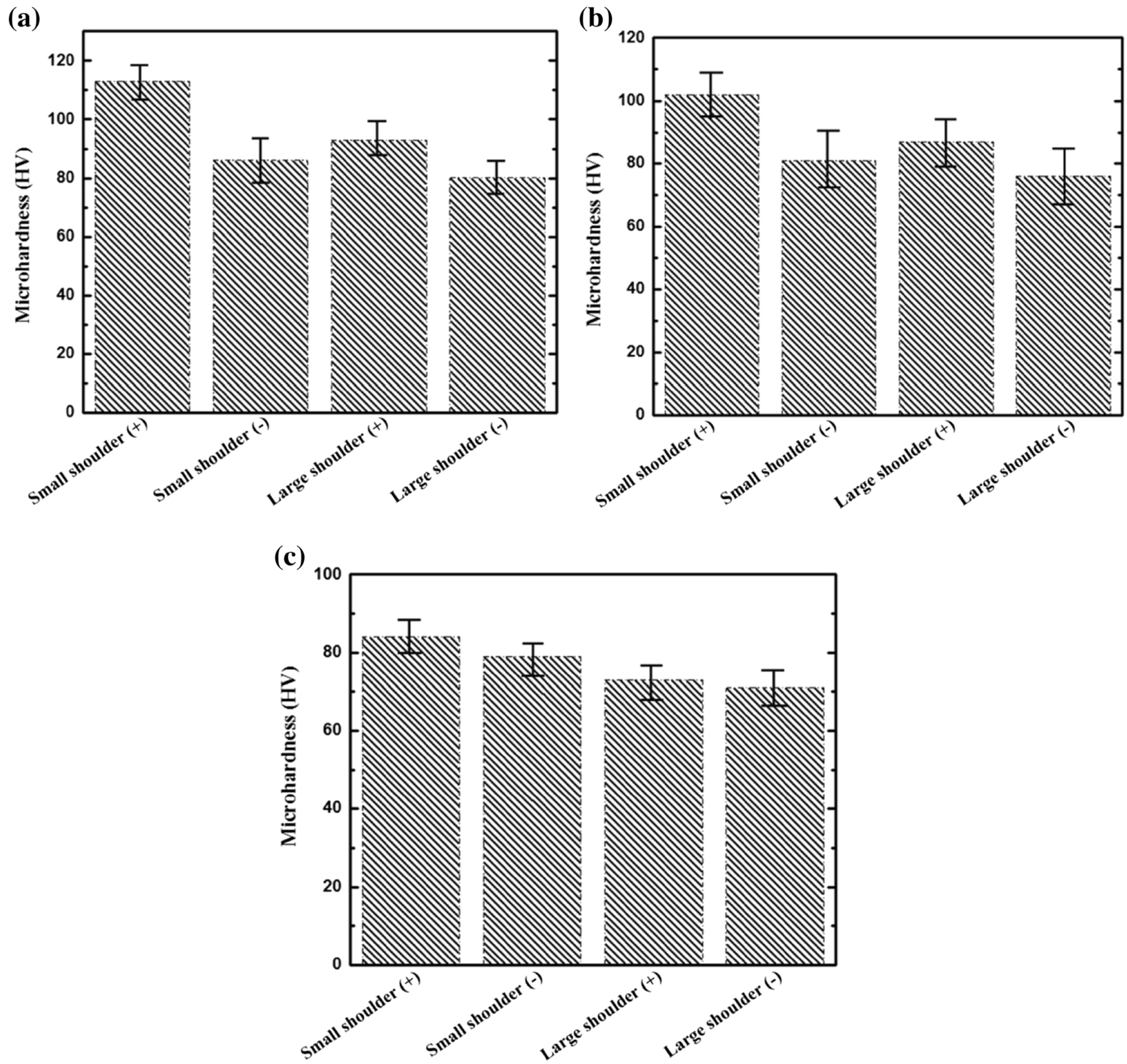


**Fig. 12** Microhardness values of different zones of FS- and FSV-welded specimens: **a** weld region, **b** TMAZ, and **c** HAZ (*minus sign* and *plus sign* denote without and with vibration, respectively)

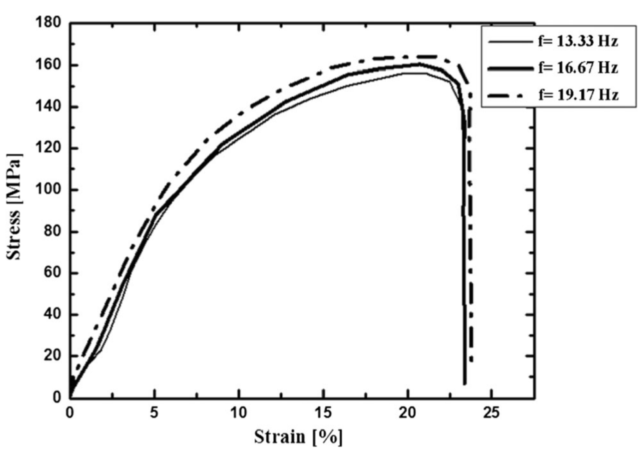


**Fig. 13** Stress-strain curves of FSV-welded specimens with different vibration frequencies

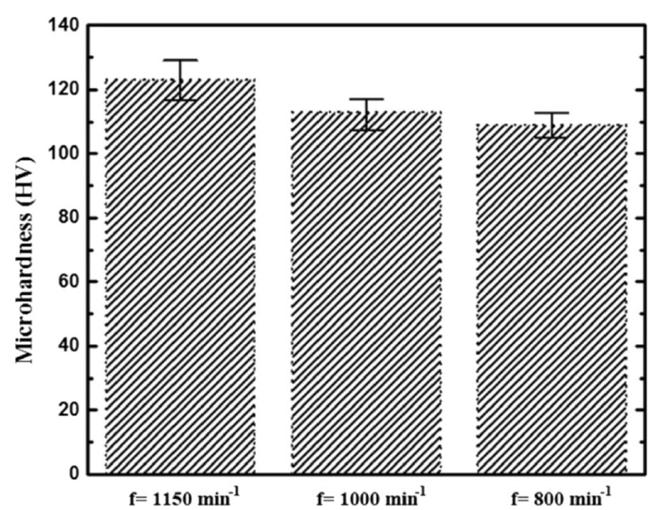


**Fig. 14** Weld region microhardness values of FSV-welded specimens

## 4 Conclusions

In the current research, a new method is presented for modification of FSW process. Workpieces are vibrated normal to weld line during rotation of shoulder and pin. In the current modified version of FSW, vibration and stirring of plasticized material in the weld region take place, simultaneously. This joining method is a friction stir vibration welding (FSVW) process. Using the presented process, Al 5052 specimens are joined together and microstructures and mechanical properties are compared with those obtained using conventional FSW process. The results show that vibration during FSW leads to grain size decrease of about 45 % in the weld region. Additionally, it is found that strength and ductility values of FSV-welded specimens are greater than those relating to FS-welded specimens (about 7 % for ultimate tensile strength and about 17 % for elongation at fracture). It is also observed that weld region microhardness of FSV-welded samples are greater than those of FS-welded samples for about 23 %. The results also indicate that increase of vibration frequency, during FSVW, increases the hardness and strength of welded specimens. It can be concluded that FSVW, as an inexpensive and easy to apply welding method, is a proper alternative process for FSW process.

## References


1. Besharati-Givi MK, Asadi P (2014) Advances in friction-stir welding and processing. Woodhead Publishing, USA
2. Davis JR (2006) Corrosion of weldments. ASM International, USA
3. Keivani R, Bagheri B, Sharifi F, Ketabchi M, Abbasi M (2013) Effects of pin angle and preheating on temperature distribution during friction stir welding operation. Trans Nonferrous Metals Soc China 23:2708–2713
4. Neto DM, Neto P (2013) Numerical modeling of friction stir welding process: a literature review. Int J Adv Manuf Technol 65: 115–126
5. Çam G (2011) Friction stir welded structural materials: beyond Al alloys. Int Mater Rev 56:1–48
6. Çam G, Mistikoglu S (2014) Recent development in friction stir welding of Al-alloys. J Mater Eng Perform 23:1936–1953
7. Mishra RS, Mahoney MW (2007) Friction stir welding and processing. ASM International, Materials Park
8. Nandan R, Debroy T, Bhadeshia HKDH (2008) Recent advances in friction stir welding process, weldment, structure and properties. Prog Mater Sci 53:980–1023
9. Mishra RS, Ma ZY (2005) Friction stir welding and processing. Mater Sci Eng R 50:1–78
10. Kohn G, Greenberg Y, Makover I, Munitz A (2002) Laser-assisted friction stir welding. Weld J 81:46–48
11. Casalino G, Campanelli SL, Contuzzi N, Angelastro A, Ludovico AD (2014) Laser-assisted friction stir welding of aluminum alloy lap joints: microstructural and microhardness characterizations. Proc. SPIE 8963, High-power laser materials processing: lasers, beam delivery, diagnostics, and applications III, 896316
12. Sun YF, Shen JM, Morisada Y, Fujii H (2014) Spot friction stir welding of low carbon steel plates preheated by high frequency induction. Mater Des 54:450–457
13. Lou J, Chen W, Fu G (2014) Hybrid-heat effects on electrical-current aided friction stir welding of steel, and Al and Mg alloys. J Mater Process Technol 214:3002–3012
14. Liu X, Lan S, Ni J (2015) Electrically assisted friction stir welding for joining Al 6061 to TRIP 780 steel. J Mater Process Technol 219: 112–123
15. Liu XC, Wu CS, Padhy GK (2015) Improved weld macrosection, microstructure and mechanical properties of 2024Al-T4 butt joints in ultrasonic vibration enhanced friction stir welding. Sci Technol Weld Join 20:345–352
16. Amini S, Amiri MR (2014) Study of ultrasonic vibrations' effect on friction stir welding. Int J Adv Manuf Technol 73:127–135
17. ASTM-E112-13 (2013) Standard test methods for determining average grain size. ASTM International, West Conshohocken
18. ASTM-E8M (2003) Standard test methods of tension testing of metallic materials [metric], Annual book of ASTM standards, vol 3.01. American Society for Testing and Materials, USA
19. Woo W, Ungar T, Feng Z, Kenik E, Clausen B (2010) X-ray and neutron diffraction measurements of dislocation density and subgrain size in a friction-stir-welded aluminum alloy. Metall Mater Trans A 41:1210–1216
20. Abbasi M, Abdollahzadeh A, Omidvar H, Bagheri B, Rezaei M (2016) Incorporation of SiC particles in FS welded zone of AZ31 Mg alloy to improve the mechanical properties and corrosion resistance. Int J Mater Res. doi:10.3139/146.111369
21. Etter AL, Baudin T, Fredj N, Penelle R (2007) Recrystallization mechanisms in 5251-H14 and 5251-O aluminum friction stir welds. Mater Sci Eng A 445-446:94–99
22. Callister WD (2007) Materials science and engineering: an introduction. Wiley, USA
23. Chang CI, Lee CJ, Huang JC (2008) Relationship between grain size and Zener–Holloman parameter during friction stir processing in AZ31 Mg alloys. Scr Mater 51:509–514
24. Mishra RS, De PS, Kumar N (2014) Friction stir welding and processing: science and engineering. Springer, London
25. Abbasi M, Abdollahzadeh A, Bagheri B, Omidvar H (2015) The effect of SiC particle addition during FSW on microstructure and mechanical properties of AZ31 magnesium alloy. J Mater Eng Perform 24:5037–5045
26. Abbasi M, Bagheri B, Keivani R (2015) Thermal analysis of friction stir welding process and investigation into affective parameters using simulation. J Mech Sci Technol 29:861–866
27. Sakai T, Miura H, Goloborodko A, Sitdikov O (2009) Continous dynamic recrystallization during the transient severe deformation of aluminum alloy 7475. Acta Mater 57:153–162
28. Sarkari Khorrami M, Kazeminezhad M, Kokabi AH (2012) Mechanical properties of severely plastic deformation aluminum sheets joined by friction stir welding. Mater Sci Eng A 543:243–248
29. Kaibyshev R, Shipilova K, Musin F, Motohashi Y (2005) Continous dynamic recrystallization in an Al-Li-Mg-Sc alloy during equal-channel angular extrusion. Mater Sci Eng A 396:341–351
30. Jonas JJ, Quelennec X, Jiang L, Martin E (2009) The avrami kinetics of dynamic recrystallization. Acta Mater 57:2748–2756
31. Dieter GE (1988) Mechanical metallurgy. McGraw-Hill Book Company, Singapore
32. Ma ZY, Pilchak AL, Juhas MC, Williams JC (2008) Microstructural refinement and property enhancement of cast light alloys via friction stir processing. Scripta Mater 58:361–366
33. Estrin YZ, Zabrodin PA, Braude IS, Grigorova TV, Iasev NV, Pustovalov VV, Fomenko VS, Shumilin SE (2010) Low

temperature plastic deformation of AZ31 magnesium alloy with different microstructures. Low Temperature Physics 36:1100–1112

34. Abbasi M, Shafaat MA, Ketabchi M, Haghshenas D, Abbasi M (2012) Application of the GTN model to predict the forming limit diagram of IF-steel. J Mech Sci Technol 26:345–352
35. Kalaki A, Ketabchi M, Abbasi M (2014) Thixo-joining of D2 and M2 tool steels: analysis of microstructure and mechanical properties. Int J Mater Res 105:764–769
36. Naderi M, Abbasi M, Saeed-Akbari A (2013) Enhanced mechanical properties of a hot-stamped advanced high-strength steel via tempering treatment. Metall Mater Trans A 44:1852–1861
37. Ketabchi M, Shafaat MA, Shafaat I, Abbasi M (2014) Effect of cooling rate on mechanical properties of 7075 aluminum rods extruded in semisolid state. J Eng Mater Technol 136:1–8